

Multi-material distributed recycling via Material Extrusion: rHDPE and rPET case of study

Catalina Suescun Gonzalez¹, Fabio A. Cruz Sanchez¹, Hakim Boudaoud¹, Cécile Nouvel¹,
Joshua Pearce¹

¹Université de Lorraine – ERPI – F-54000, Nancy, France

²Université de Lorraine, CNRS, LRGP, F-54000 Nancy, France

³Western University, Department of Electrical & Computer Engineering, Canada, London

Abstract

The high volume of plastic waste and the extremely low recycling rate have created a serious challenge worldwide. Local distributed recycling coupled with additive manufacturing (DRAM) offers a solution by economically incentivizing local recycling. One DRAM technology capable of processing large quantities of plastic waste is fused granular fabrication (FGF), where solid shredded plastic waste can be reused directly as 3D printing feedstock. This study presents an experimental assessment of multi-material recycling printability using two of the most common thermoplastics in the beverage industry, polyethylene terephthalate (PET) and high-density polyethylene (HDPE), and the feasibility of mixing PET and HDPE to be used as a feedstock material for large-scale 3-D printing. After the material collection, shredding, and cleaning, the characterization and optimization of parameters for 3D printing were performed. Results showed the feasibility of printing a large object from rPET/rHDPE flakes, reducing the production cost by up to 88%.

Acronyms

Acronym	Definition
ABS	Acrylonitrile Butadiene Styrene
AM	Additive Manufacturing
DRAM	Distributed recycling via additive manufacturing
DSC	Differential scanning calorimetry
FDM	Fused deposition modeling
FFF	Fused filament fabrication
FGF	Fused granular fabrication
FPF	Fused particle fabrication
FTIR	Fourier-transform infrared spectroscopy
HDPE	High-density polyethylene
MFI	Melt flow index
PC	Polycarbonate
PET	Poly(ethylene terephthalate)
PLA	Poly(lactic acid)
PP	Polypropylene
PSO	Particle swarm optimization
PS	Polystyrene
SEBS	Poly (styrene-block-ethene-co-butene-block-styrene)
Tg	Glass temperature
pBC	Printed Bottle-Cap
rHDPE	Recycled High-density Polyethylene
rPET90//rHDPE10	Recycled Bottle-Cap (Cristaline bottle shredded without separation)
rPET	Recycled Poly(ethylene) terephthalate
vPET	Virgin or commercial Poly(ethylene terephthalate)

Introduction

- 1 The disposal of plastic waste is one of the most challenging current environmental concerns given its systemic
2 complexity ([Evode et al., 2021](#)). The mass of micro- / meso- plastics in the oceans is expected to exceed
3 the mass of the global stock of fish by 2050 ([MacArthur, 2017](#)). More critically, the global annual plastic
4 production is expected to reach 1100 metric tons by the same year ([Geyer, 2020](#)). Societal awareness of plastic
5 recycling has received substantial attention from scientists, policymakers, and the general public ([Soares et](#)
6 [al., 2021](#)). Unfortunately, the statistical analysis of the centralized recycling process proves that it has been
7 largely ineffective ([Siltaloppi and Jähi, 2021](#)) with only 9% of the plastic produced since 1950 being recycled
8 from the total stock ([Geyer et al., 2017](#)). Therefore, it remains an open challenge to identify alternatives to
9 valorize discarded plastic material.
- 10 Distributed recycling and additive manufacturing (DRAM) is an innovative technical approach to recycling
11 plastic waste ([Cruz Sanchez et al., 2020; Dertinger et al., 2020](#)). DRAM was initially implemented using
12 recyclebots, which are waste plastic extruders that produce filament for conventional fused filament-based

13 3-D printers (Baechler et al., 2013; Woern et al., 2018; Zhong and Pearce, 2018). Previous studies have
14 shown that distributed recycling aligns with the circular economy paradigm (Despeisse et al., 2017; Ford
15 and Despeisse, 2016). This approach allows consumers to directly recycle their own waste into consumer
16 products using open-source designs, ranging from toys for children (Petersen et al., 2017) to adaptive aids
17 for individuals with arthritis (Gallup et al., 2018). Distributed manufacturing is now widely adopted (Pearce
18 and Qian, 2022). In this way, DRAM-based recycling operates within a closed-loop supply chain network
19 (Santander et al., 2020). The primary goal of this type of recycling is to reduce the environmental impact by
20 minimizing the transportation from the waste source to recycling facilities (Kreiger et al., 2014). In that sense,
21 it aims to propose innovative closed-loop strategies that utilize waste materials as raw resources (Romani et
22 al., 2021).

23 Fused filament fabrication (FFF, which is also known as Fused Deposition Modelling –FDM©-) is the most
24 widespread and established extrusion-based AM technology. It has gained popularity due to the open-source
25 proliferation from the self-replicating rapid prototyper (RepRap) project (Bowyer, 2014; Jones et al., 2011;
26 Sells et al., 2009). FFF is favored for its simplicity, versatility, low cost, and ability to construct complex
27 geometric objects in the industrial and prosumer domains (Romani et al., 2021). Indeed, the open-source
28 approach for 3-D printing has facilitated significant advancements in manufacturing and prototyping adding
29 value to the recycled material (Cruz Sanchez et al., 2020). Efforts are being made to identify sustainable
30 feedstocks for 3-D printing Pakkanen et al. (2017a). Several studies have expanded the range of recycled
31 filament materials including PLA (Anderson, 2017; Cruz Sanchez et al., 2017), ABS (Mohammed et al.,
32 2017b, 2017a), PET (Vaucher et al., 2022; Zander et al., 2018), HDPE (Baechler et al., 2013; Chong et al.,
33 2017; Mohammed et al., 2017b), and PC (Gaikwad et al., 2018). In fact, Kreiger et al. (2014) conducted a
34 comparative life cycle assessment in a low-density population case study in Michigan (USA) and estimated
35 that a distributed approach could save approximately 100 billion MJ of energy per year from the recycling of
36 984 million pounds of HDPE. There is substantial evidence that DRAM can contribute to reducing energy
37 consumption and greenhouse emissions in manufacturing processes.

38 Most DRAM studies have used mono-materials for the fabrication of feedstock for FFF. There are, however,
39 several examples of mixed materials including wood waste and recycled plastic (Löschke et al., 2019; Pringle et
40 al., 2018) and textile fibers and recycled plastic (Carrete et al., 2021). Recently, Zander et al. (2019) reported
41 the manufacturing of composite filament from recycled PET/PP and PS/PP blending through a compati-
42 bilizer copolymer such as SEBS. Their results revealed the technical printability of polypropylene blend
43 composite filaments from a thermo-mechanical characterization perspective. Increasing the performance win-
44 dow of blending materials by compatibilization which could be a relevant path for recycling plastics at a local
45 level and in isolated areas contexts (e.g. during humanitarian crises (Corsini et al., 2022; Lipsky et al., 2019;

46 Savonen et al., 2018), supply chain disruptions (Attaran, 2020; Choong et al., 2020 ; Novak and Loy, 2020;
47 Salmi et al., 2020) and/or isolated off-grid situations using solar-powered 3-D printers (Gwamuri et al., 2016;
48 King et al., 2014; Mohammed et al., 2018; Wong, 2015)). Likewise, Vaucher et al. (2022) studied the evalua-
49 tion of the microstructure, mechanical performance, and printing quality of filaments made from rPET and
50 rHDPE varying the wt% of HDPE material from 0 to 10%. They confirmed the increase in Young's modulus
51 from 1.7 GPa of the pure PET to 2.1 GPa for all the HDPE concentrations. Additionally, the maximum
52 stress of the bends was augmented with high HDPE concentrations. Values were lower than virgin PET
53 filament, yet similar to commercial recycle ones. The addition of rHDPE at higher levels, however, helped to
54 meet the brittle-ductile transition in 15% despite the low interfacial tension of both polymers, allowing the
55 printing of quality parts.

56 While former studies have proven successful in FFF, a new approach to DRAM is fused granular fabrication
57 (FGF) or fused particle fabrication (FPF), where the material-extrusion AM systems print directly from
58 pellets, granules, flakes, shreds or grinder material (Fontana et al., 2022; Woern et al., 2018). In the context
59 of recycling, this could reduce the number of melt/extrusion cycles that degrade the material needed in
60 the filament fabrication process (Cruz Sanchez et al., 2017). The FGF technique opens up the potential to
61 use recycled materials as well as print large-scale objects either with a conventional cartesian 3-D printer
62 (Woern et al., 2018), delta 3-D printer (Grassi et al., 2019) or hangprinter (Petsiuk et al., 2022; Rattan
63 et al., 2023). Research groups have corroborated that plastic waste can be used as feedstock materials for
64 FGF/FPF. Alexandre et al. (2020) assessed the technical and economical dimensions of virgin and shredded
65 PLA printed in a self-modified FGF machine and compared it with FFF. The investigation showed that the
66 use of FGF reduced printing costs, time and its mechanical performance was comparable to that obtained
67 using the traditional FFF technique. Likewise, Woern et al. (2018) found comparable properties between
68 PLA, ABS, PP, and PET recycled and virgin materials. Later publications demonstrated the technical and
69 economic feasibility through the printing of complex objects validating the possibility of recycling plastic with
70 FGF in both conventional and common FFF materials (Byard et al., 2019), but also recycling PC (Reich et
71 al., 2019) and rPET (Little et al., 2020). Few researchers, however, have addressed the problem of directly
72 printing recycled multi-materials, which might be a key step forward needed to facilitate the ease of sorting
73 and recycling post-consumer plastic waste materials.

74 This study explores the potential of direct 3-D printing of two immiscible polymers commonly used in the
75 beverage sector through a distributed recycling process for its easy implementation operation at the local
76 level. To demonstrate the feasibility of the process, the most commonly used plastic for bottled water in
77 France, which consists of roughly 90% PET (body of the bottle) and 10% HDPE (cap) now referred to as
78 rPET90//rHDPE10, is used as a test material. The experimental process of collection, characterization, and

79 printing of the recycled material is described, and the results are discussed in the context of widespread
80 DRAM adoption at the community-based level.

81 Materials and Methods

82 The methodology presented in Figure 1 outlines the approach adopted to develop the study. The three stages,
83 namely *Material obtention*, *Printing process*, and *Evaluation* were thoroughly studied to control the major
84 process steps and the technical characterization methods. In the following subsections, each step is explained.

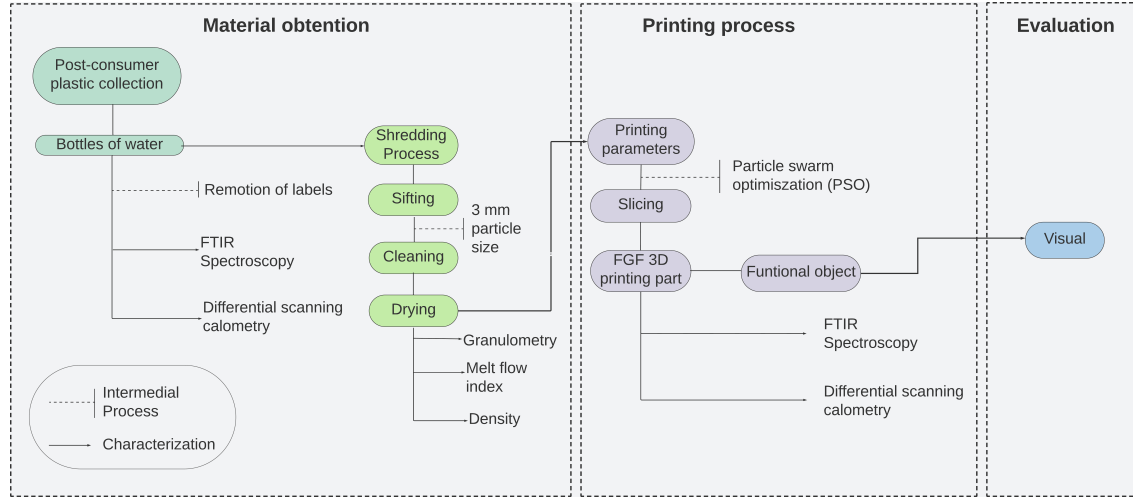


Figure 1: Global framework of the study

85 Raw material obtention

86 The goal of the material stage is to collect and prepare post-consumer plastic sources. In this study, water
87 bottles coming from the French brand Cristaline[®] were used as feedstock. The process steps used are shown in
88 Figure 2 a/b. Post-consumer bottles were collected from receptacles placed in partnership schools in Lorraine,
89 France. To convert the complete water bottles including their caps into 3DP feedstock material, the labels
90 were removed before shredding in a cutting mill (Retsch MS300) using a 3 mm grid. After shredding, the
91 obtained flakes were sifted with a 1.5 mm, 3 mm, and 5 mm sifters for further analysis. Next, the flakes
92 were cleaned with hot water in an ultrasonic machine at 60°C for 1 hour to remove contaminants. Lastly,
93 they were dried in a conventional oven overnight at 80°C (Taghavi et al., 2018; Van de Voorde et al., 2022)
94 to avoid degradation of the material. Washing conditions were the same for all the samples; therefore, the
95 effect of contaminants was not considered. The resultant material is shown in Fig 2.c.

96 The material composition was calculated as a function of the mass of the bottles and caps separately. The

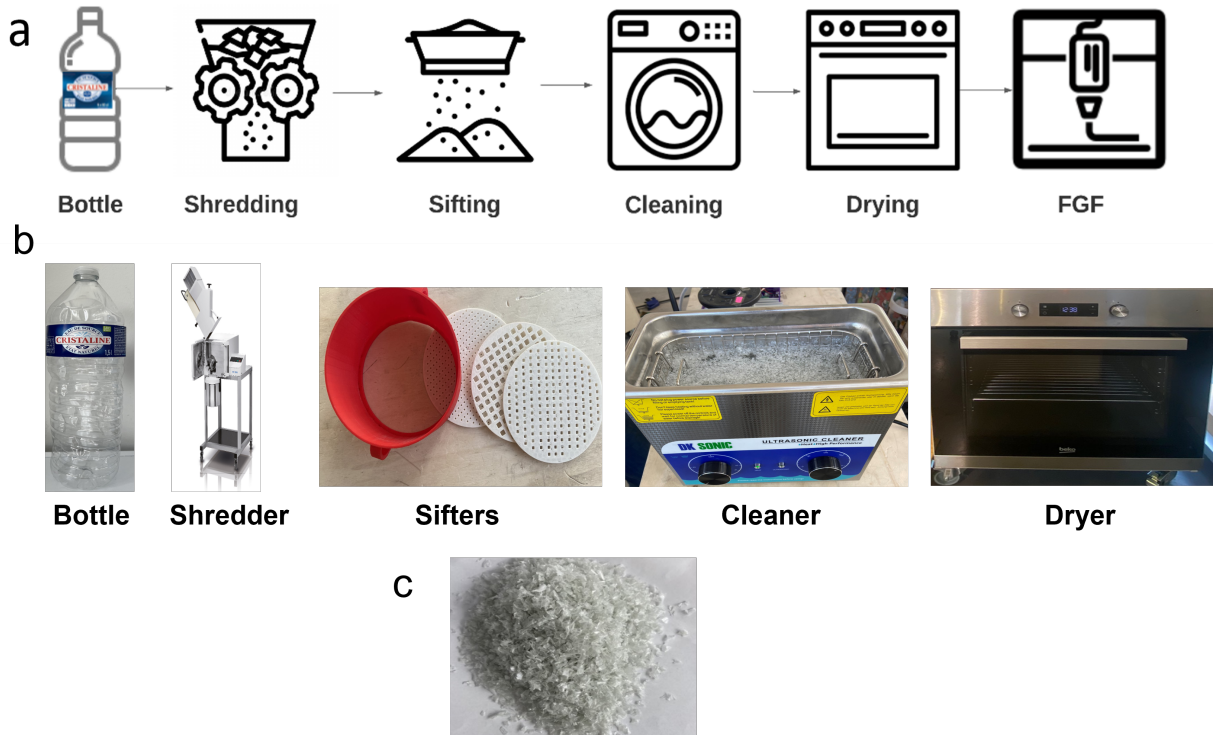


Figure 2: Process steps to prepare the collected material

percentage (%) of bottle-cap was found to be ~90%rPET (bottle) and ~10% rHDPE (cap). The complete bottle was shredded without separation of both materials thus this percentage is constant for all the samples.

Material preparation and characterization

Material particle size analysis -Granulometry-

In order to ensure the particle size suitable for printing, the granulate particles were characterized using the open-source ImageJ software (ImageJ, 2023). The size characteristics of the particles were evaluated in four different samples: vPET (used as a reference) and the raw material sifted into three different sizes: 1.5 mm, 3 mm, and 5 mm.

Fourier-transform infrared spectroscopy –FTIR–

FTIR spectroscopy was conducted to determine the composition of the bottle and identify any impurities, plasticizers, or additives. The analysis involving testing separate samples of rPET and rHDPE. Additionally, a printed sample of both materials was examined to identify any potential chemical bonding. Each sample was measured at two different points, with three measurements taken at each point. The resulting curves were

110 then normalized and analyzed using Origin Pro 8. The Fourier transform infrared spectra were recorded in
111 the range of 4000 cm^{-1} to 375 cm^{-1} with a resolution of 4 cm^{-1} using a Bruker IFS 66V spectrophotometer.

112 **Differential scanning calorimetry –DSC–**

113 Differential scanning calorimetry analysis was performed using a DSC-1 Mettler Toledo with STARe software
114 operating under nitrogen atmosphere at heating rate and cooling rate of $10\text{ }^{\circ}\text{C/min}$. The samples investigated
115 were rPET, rHDPE, and rPET90//rHDPE10. Three cycles were conducted: the first involved heating from
116 $20\text{ }^{\circ}\text{C}$ to $270\text{ }^{\circ}\text{C}$, cooling to $20\text{ }^{\circ}\text{C}$ and reheating to $270\text{ }^{\circ}\text{C}$. The rHDPE sample was analyzed using similar cycles
117 but with the maximum temperature set at $250\text{ }^{\circ}\text{C}$ and the blend was tested at temperatures ranging from
118 -20 to $270\text{ }^{\circ}\text{C}$. The glass transition temperature (T_g) of rPET was determined during the first heating cycle,
119 while the T_g of rPET90//rHDPE10 was determined during the second heating cycle, along with the melting
120 point of all materials. The crystallization temperature (T_c) was determined during the cooling cycle for each
121 material. The degree of crystallinity (X_c) was calculated from the second cycle for recycled materials and
122 the first cycle for the blend, as expressed in equation (1) (Pan et al., 2020; Taghavi et al., 2018):

$$X_c(\%) = \frac{\Delta H_m}{w \cdot \Delta H_m^{\circ}} \quad (1)$$

123 Where, ΔH_m is the latent heat of melt, w is the weight percentage of polymer in the blend, and ΔH_m° is
124 the reference heat of 100% crystalline PET (140 J/g) and HDPE (293 J/g), respectively, provided in the
125 literature (Kratofil et al., 2006; Pan et al., 2020).

126 **Melt Flow Index –MFI–**

127 The melt-flow index (MFI) of rPET90//rHDPE10 flakes was determined using an Instron CEAST MF20.
128 The analysis was performed using three samples of $\sim 5\text{ g}$ at a temperature of $255\text{ }^{\circ}\text{C}$ with a 2.16 kg weight
129 following the ASTM D1238 standard. The process was repeated three times. The average value of the three
130 results was reported in units of $gr/10 \times min$.

131 **Density**

132 The material's density was calculated as follows: first, the volume was found by measuring the dimensions of
133 a solid $50 \times 50 \times 50\text{ mm}$ cubic geometry fabricated by injecting rPET90//rHDPE10 flakes into a square mold
134 with a known volume using an open-source desktop injection machine(Holipress, Holimaker, France). Then,
135 the model was weighed, and the mass was obtained. Finally, the density was calculated as expressed in
136 Equation 2. To ensure the accuracy of the test it was performed twice and the average value was reported

¹³⁷ in g/cm^3 .

$$\rho = V/m \quad \left[\frac{g}{cm^3} \right] \quad (2)$$

¹³⁸ Where, ρ is the density, V is the volume, and m the mass.

¹³⁹ Afterwards, experimental results were compared with the theoretical blend density which could be calculated
¹⁴⁰ by Equation 3.

$$\rho_{12} = \frac{1}{\frac{W_1}{\rho_1} + \frac{W_2}{\rho_2}} \quad \left[\frac{g}{cm^3} \right] \quad (3)$$

¹⁴¹ Where, ρ_{12} is the density of the blend, W_1 and W_2 , the weight fractions of each polymer, ρ_1 and ρ_2 , the theo-
¹⁴² retical density of each polymer for PET ($1.38 g/cm^3$) and HDPE 0.93 to $0.97 g/cm^3$ ([Jonathan GUIDIGO1 et al., 2017](#)).
¹⁴³

¹⁴⁴ Printing process

¹⁴⁵ Establishing optimal parameters

¹⁴⁶ Establishing the optimal combinations of parameters is essential for improve the quality and mechanical
¹⁴⁷ properties of printed parts ([Jaisingh Sheoran and Kumar, 2020](#)). According to Oberloier et al. (2022a),
¹⁴⁸ particle swarm optimization (PSO) is an accurate and time-effective method for achiving this goal. To
¹⁴⁹ optimize the 3-D printing parameters for the rPET90//rHDPE10 material in the GigabotX we utilized
¹⁵⁰ the open-source PSO Experimenter platform which is available for Linux. The methodology developed by
¹⁵¹ Oberloier et al. (2022a) was followed during the optimization. For benchmarking purposes, three artifacts
¹⁵² were printed: a line, a plane, and a cube. These artifacts were modeled in CAD software Onshape CAD
¹⁵³ v1.150 and sliced using Prusaslicer v2.52.0. Figure 3 presents the geometry models and dimensions of the
¹⁵⁴ artifacts.

¹⁵⁵ Four parameters were assessed: 1) nozzle temperature, 2) bed temperature, 3) printing speed and 4) extrusion
¹⁵⁶ multiplier ([Oberloier et al., 2022b](#)). The initial parameters for the line are presented in Table 1a while
¹⁵⁷ additional parameters were obtained from preliminary experimental work shown in Table 1.b. Finally, the
¹⁵⁸ PSO tuning parameters were found in the previous PSO work ([Oberloier et al., 2022a](#)) Table 1.c.

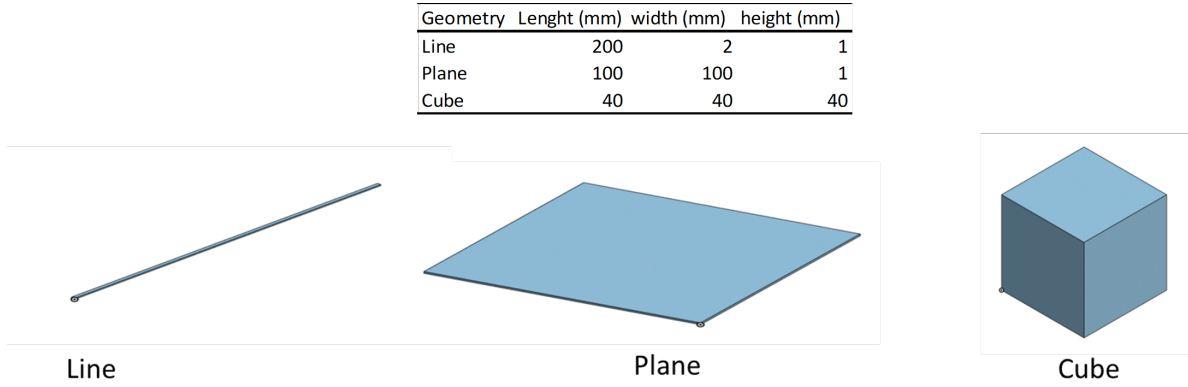


Figure 3: Dimensions and CAD models of the geometries used for parameters optimization.

Table 1: table 1

(a) Line optimization initial parameters

Variable	Min	Max	Guess	True/False	Description
T1	255	270	260	TRUE	Temperature Zone 1 on GigabotX
Tb	80	90	85	TRUE	Bed temperature
Ps	10	25	15	TRUE	Printing Speed
E	0.5	2	1	FALSE	Extrusion Multiplier

(b) Fixed parameters to perform printing parameters optimization based on PSO

Parameters	Value	Units
Layer height	0.5	mm
Width	2	mm
T2	230	°C
T3	220	°C
Cooling	0	%
Infill density	2	%

(c) Recommended parameters for PSO tuning

Variable	Value	Description
Kv	0.5	The emphasis given to the velocity component
Kp	1.0	The emphasis given to a particle's personal best position
Kg	2.0	The emphasis given to the swarm's group's best position

159 **Fused Granular Fabrication –FGF-**

160 To print the obtained raw material, a modified open-source printer with three heat zones (Gigabot XL re:3D,
161 Houston, TX, USA) was utilized as illustrated in Figure 4. The machine is a single screw extrusion-based
162 3-D printer capable of direct printing pellets, flakes, or granules, with a nozzle size of 1.75 mm. For this
163 study, a chair was printed to evaluate the material's ability to be 3-D printed and the printer's capability to
164 produce large objects like furniture. The ideal parameters determined for the cube geometry were employed
165 to print the final part.

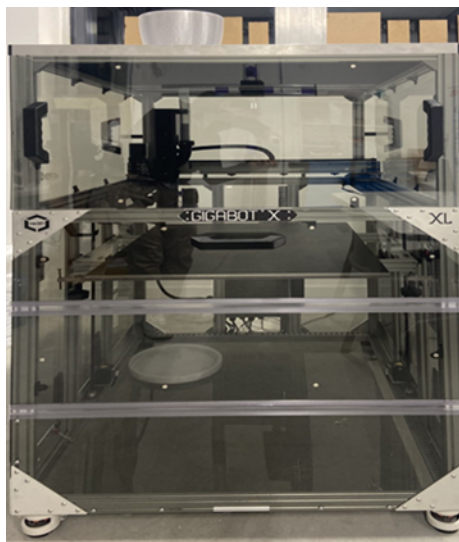


Figure 4: Fused granular fabrication printer Gigabot

166 **Results and discussion**

167 **Material characterization**

168 Both the polymeric components of the bottle and the blend were characterized and analyzed to determine
169 their properties using different methods as described in the preceding section.

170 **Material particle size analysis (granulometry)**

171 Previous studies demonstrated that particles with areas smaller than 22 mm^2 were optimal for printing
172 without experiencing jamming or under-extrusion problems (Woern et al., 2018). However, our experiments
173 revealed that particles with areas exceeding 10 mm^2 caused clogging in the feeding system and auger screw
174 of the machine. As a result, granulometry analysis was performed using three different mesh sizes.

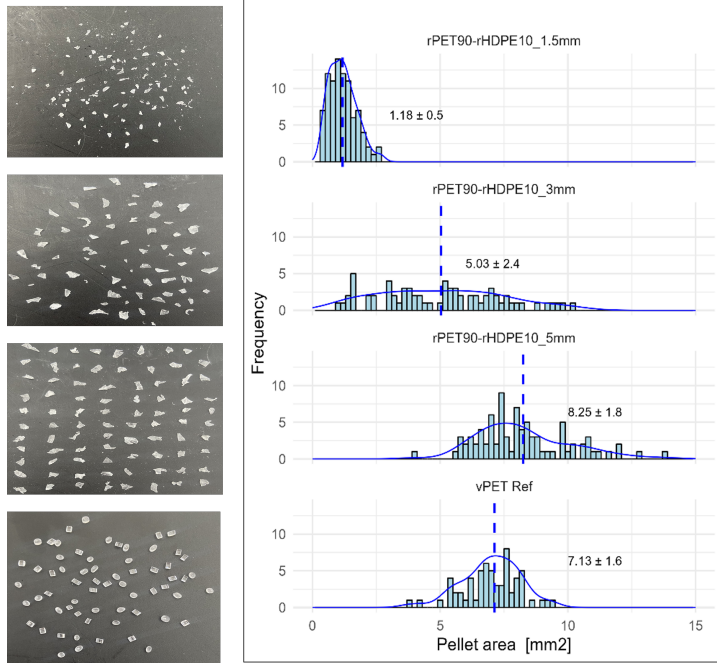


Figure 5: Granulometry analysis

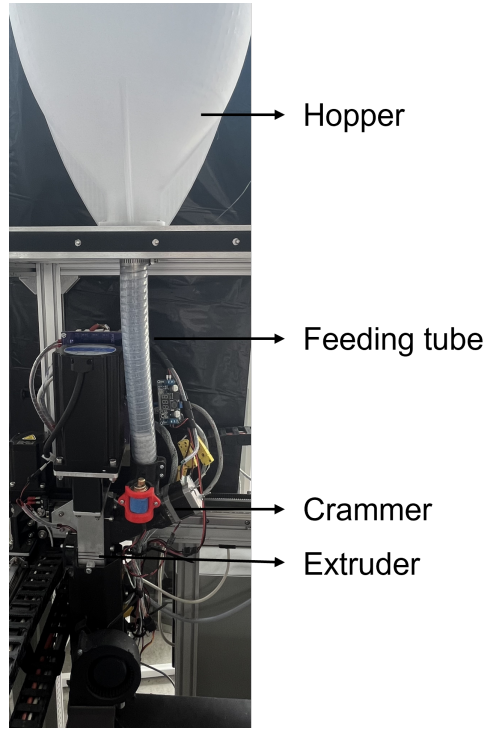


Figure 6: Gigabot feeding system

175 Figure 5 presents the obtained results, indicating that particles sifted at 5 mm exhibited an average area
 176 similar to the reference. There are, however, particles with areas exceeding 9 mm^2 caused blockages in
 177 the feeding and extrusion section. Particles sifted to 1.5 mm displayed a distribution ranging from 0 to
 178 approximately 3 mm^2 , which was deemed too small for printing purposes. The presence of these small
 179 particles can lead to their complete melting in the initial heat zone, thereby impeding the smooth flow of
 180 other particles and preventing the necessary pressure for extruding the melted particles further down the
 181 screw. Although flakes measuring 3 mm exhibited a more dispersed distribution and slightly smaller area
 182 compared to the reference, they were found to be optimal for printing.

183 The final objects, however, still showed under-extrusion issues. To address this problem, a crammer was
 184 implemented (Little et al., 2020) as presented in Figure 6. The crammer physically pushes particles towards
 185 the auger, facilitating their transfer from the feeding tube to the extruder. After the crammer implementation
 186 the under-extrusion issues were greatly reduced. It was concluded that flakes with areas ranging from 1.5 mm^2
 187 to 10 mm^2 were the most suitable for printing when using a crammer to assist the feeding system.

188 **Chemical analysis from FTIR**

189 Chemical structure information of the materials was obtained using FTIR spectroscopy, which allowed the
190 analysis of the characteristic spectral bands of the polymers.

191 In the case of rPET (bottle) four distinct bands can be observed in Figure 7. The first band, located at
192 1713cm^{-1} represent the $C = O$ double bond. The second band, at 1240cm^{-1} , corresponds to the $C - O$
193 single bond ester. The third band, at 1093cm^{-1} , is associated with band the methylene group and vibrations
194 of the ester bond. Lastly, a band at 722cm^{-1} which represents the CH_2 rocking bending vibration. Similar
195 results were reported in the literature for PET derived from recycled water bottles, soda bottles, and food
196 containers (Zander et al., 2018).

197 Regarding rHDPE (caps), four characteristic peaks were identified: the C-H functional group bond at
198 2915cm^{-1} and 2847cm^{-1} , the primary bending mode of the $-\text{CH}_2$ at 1465cm^{-1} and the CH_2 rocking
199 bending vibration at 729cm^{-1} . The results obtained confirmed the chemical structures of the starting mate-
200 rials. Additionally, no other indicative resonances, apart from those associated with the polymer structures
201 were detected. This leads to the conclusion that there were no significant amounts of additives or plasticizers
202 present in either of the samples. Moreover, the spectrum of the printed blend (rPET90//rHDPE10) exhibited
203 identical characteristic peaks to those observed in the bottle, thus confirming the predominant presence of
204 PET. There are, however, noticeable differences between 1000cm^{-1} and 720cm^{-1} as well as in the C-H
205 bond (2915cm^{-1} and 2847cm^{-1} peaks), which confirm the presence of HDPE (cap). The observed shift can
206 be attributed to interactions between the two materials.

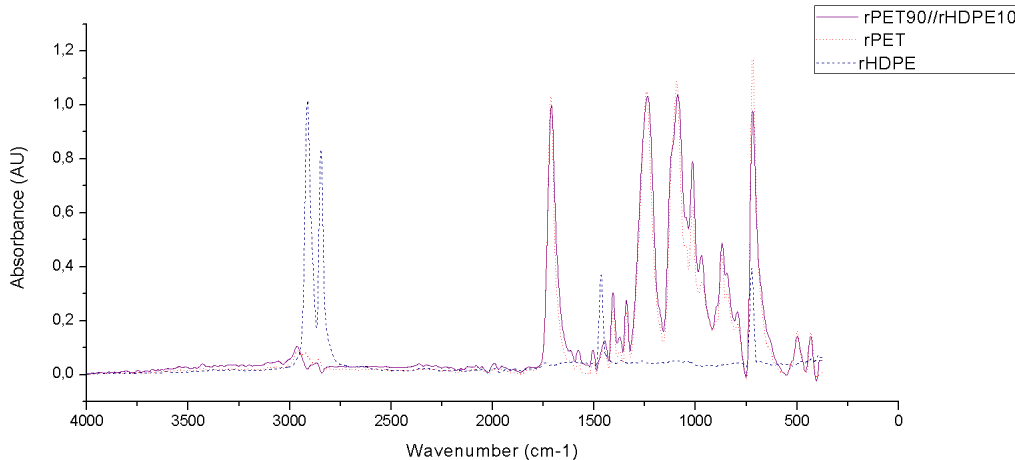


Figure 7: FTIR spectra of rPET, rHDPE, and their blend

Table 2: Thermal analysis of rPET, rHDPE, and their blend

Sample	Glass transition		Melting		Crystallization			% Crystallinity
	Tg (°C)		Tm (°C)	ΔHm (J/g)	Tc (°C)	ΔHc (J/g)	ΔHcc (J/g)	
rPET	82		249.9	32.3	196.7	33.3	-	23.1
rHDPE	-		133.8	172	118.7	158.2	-	58.7
rPET90/rHDPE10	77 / -		254/131.7	40.3/1.30	210.6/117.4	37.9/6.7	6.8	26.6 / 18.8

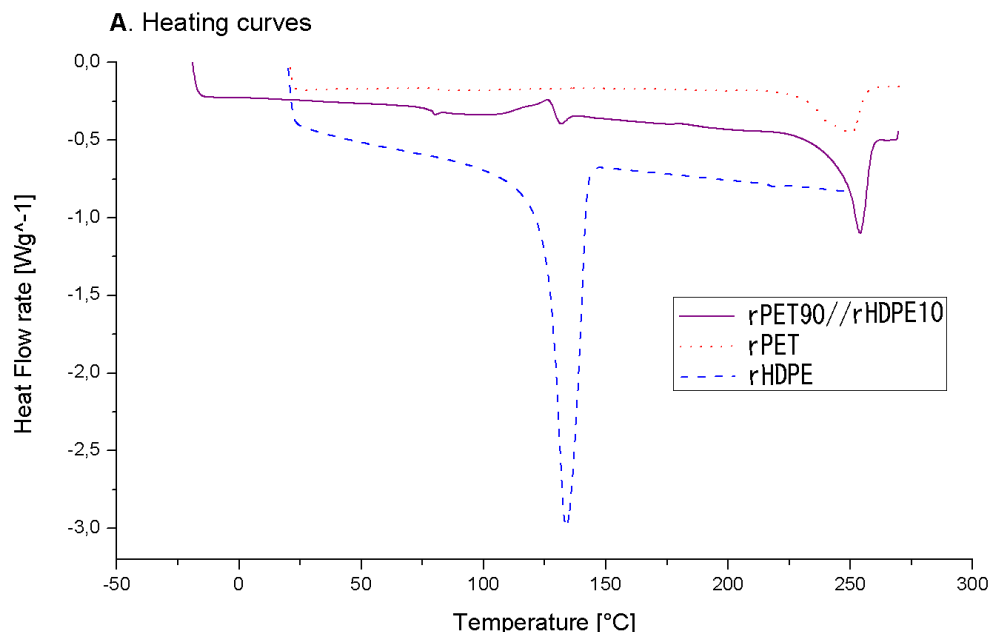
207 Thermal analysis DSC

208 The thermal properties of both recycled materials and their blend were characterized using DSC to establish
 209 a baseline for optimizing process parameters of 3-D printing.

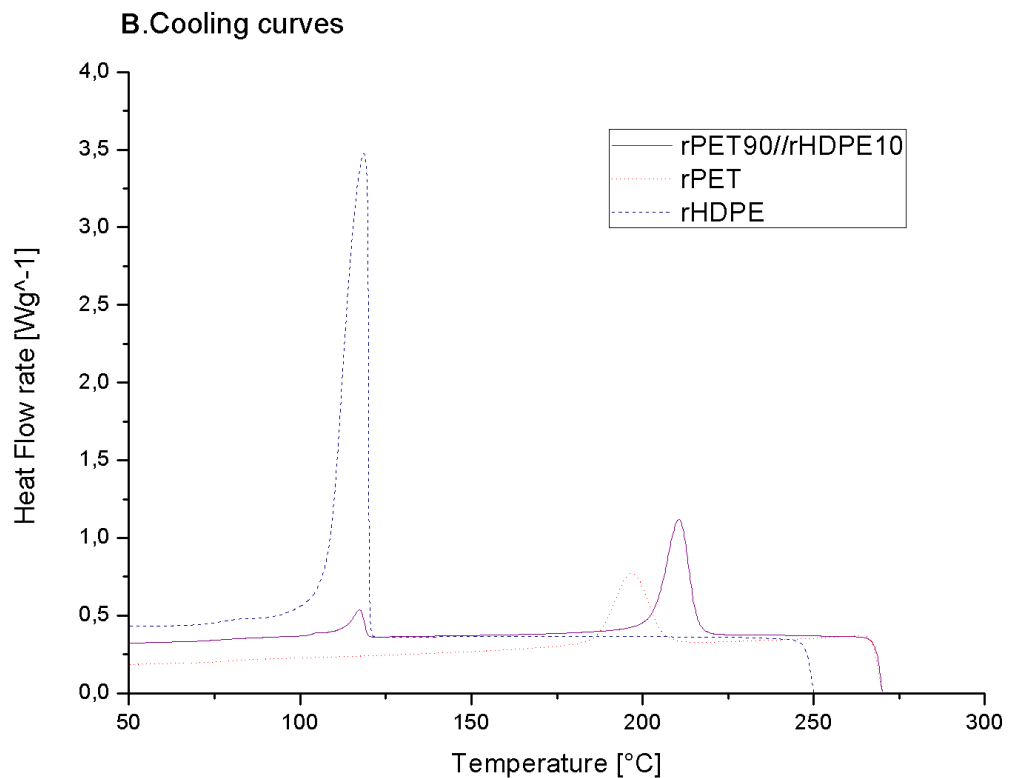
210 Two distinct endothermic peaks are observed in the representative heating and cooling thermograms shown in
 211 Figure 8, for the printed blend sample. These peaks are associated with the fusion of the crystalline fractions
 212 of rHDPE and rPET, providing confirmation of the immiscibility of both materials. Moreover, the enthalpy
 213 of fusion and crystallization of the rHDPE in the blend is significantly reduced, which can be attributed to
 214 the low percentage of HDPE present in the blend. Furthermore, the presence of a cold crystallization peak
 215 in the blend, but not in the individual polymers, suggests an interaction between the two polymers. It is
 216 possible that the rHDPE acts as a nucleating agent in this interaction. Table 2 lists the thermal properties of
 217 rPET, rHDPE and rPET90//rHDPE10. The melting points of rHDPE and rPET are 131.7 °C and 249.9 °C,
 218 respectively, which align with previous findings in the literature ([Chen et al., 2015](#); [Lei et al., 2009](#); [Vaucher et al., 2022](#)). It is observed that the melting and crystallization temperature of rPET increased, while that
 219 of rHDPE slightly decreased. Furthermore, the crystallization of rPET was found to be somewhat affected
 220 by the presence of rHDPE, resulting in a 3.5% increase in degree of crystallization. This can be attributed
 221 to the rHDPE acting as a germination point for crystallization ([Vaucher et al., 2022](#)). The slight changes in
 222 the fusion-crystallization temperatures and degree of crystallinity of rPET indicate an interaction of both
 223 polymers.

225 Rheology MFI

226 The melt flow index of the flakes was determined, enabling a fast and practical screening of the viscosity of
 227 the material. Based on the DSC results, the initial temperature for the MFI test was 250°C. However, the
 228 material did not flow reliably at this temperature, so it was increased by 5°C to enable the determination of
 229 the melt flow index of the rPET90//rHDPE10 blend. A temperature of 260°C was also tested, however, the
 230 material flowed too rapidly, making it difficult to obtain reliable measurements. The MFI tests were performed
 231 three times and the results for the rPET90//rHDPE10 blend showed medium MFI of 39.4 ± 2.4 g/10min.
 232 This value is consistent with similar values reported in the literature for rPET ([Bustos Seibert et al., 2022](#);



(a) Heating curves



(b) Cooling curve

Figure 8: DSC thermograms of recycled materials and blends ¹⁴

233 Langer et al., 2020; Nofar and Oğuz, 2019). This result suggest that addition of low percentage of HDPE
234 does not significantly impact the MFI value of rPET. Since the material flowed at a temperature of 255°C in
235 the MFI test, this temperature was used as the input temperature for optimizing the parameters of the 3-D
236 printer.

237 **Density**

238 The density provides valuable information for estimating the cost, material usage, time consumption, and
239 weight of the printed object in the slicer. This information is useful to determine the accurate printing
240 parameters using the PSO experimenter, as the fitness of the object is calculated based on its dimensional
241 accuracy and weight. Hence, density plays a significant role in determining the weight of the geometries.

242 After conducting calculations and measuring the rPET90//rHDPE10 injected object, it was determined that
243 the density of the material is 1.13 g/cm^3 . The inclusion of HDPE in the matrix polymer resulted in a slight
244 decrease in density, which is a common occurrence when a polymer is mixed with a lower-density polymer.
245 However, if we consider a PET/HDPE blend with a mass ratio of 90/10, the calculated theoretical density
246 would be 1.32 g/cm^3 . The observed decrease of 14% in the results could be attributed to factors, such as
247 experimental conditions and manual measurements.

248 **Particle swarm optimization (PSO) Experimenter**

249 Geometries were 3-D printed by adjusting the parameters using the PSO Experimenter software. The fit-
250 ness function is defined by the weighted sum of the dimensional measurements (length, width, height, and
251 weight) of the printed object. A fitness value below 0.1 was consider desirable. In the software five particles
252 were established for each iteration, resulting in five different parameter combinations being printed in each
253 iteration.

254 After six iterations and a total of thirty lines printed, the first geometry (line) achieved a fitness value of less
255 than 0.1. The optimal parameters for this geometry are listed in column two of Table 3 and images of the
256 resulting geometries are illustrated in Figure 9 .

257 Afterwards, these parameters were used as initial guesses for plane geometry, which achieved the desired
258 fitness in the first iteration. Similarly, cubes were printed using the plane ideal parameter as the initial
259 guess, and optimal parameters, were found in the first iteration. The results showed a significant decrease
260 in printing speed, as the geometry complexity increased. Moreover, the cube geometry required a higher
261 extrusion multiplier to fill gaps and overcome under-extrusion problems. The optimization of parameters
262 for the three geometries took approximately 10h reducing the experimental time, compared to conventional

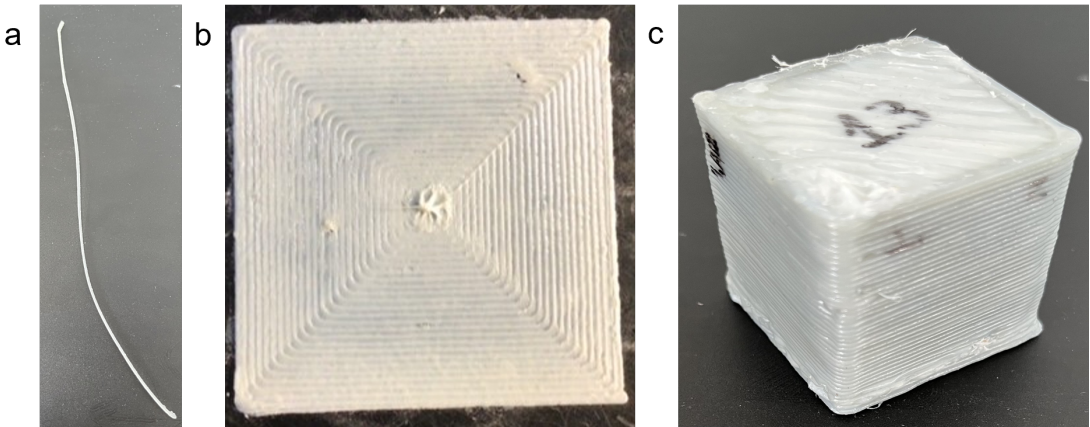


Figure 9: Images of the resulting geometries a) line, b) plane, c) cube

263 methods. According to Oberloier et al. (2022a), this experimentation time can be reduced by 97%. Indeed,
 264 the effectiveness of PSO in finding global optimum parameters is high, especially in cases with a large or
 265 complex design space (Saad et al., 2019; Selvam et al., 2020).

266 Additionally, PSO converge to optimum solutions with fewer iterations than DoE methods (Zhang et al.,
 267 2015). Combining PSO with other meta-heuristic methods has demonstrated higher ability to predict and
 268 optimize parameters (e.g. minimize surface roughness(Shirmohammadi et al., 2021), compressive strength and
 269 porosity of scaffolds (Asadi-Eydivand et al., 2016), and mechanical properties(Raju et al., 2019)). However,
 270 DoE methods are still widely used as they provide insight into the effects of individual design parameters and
 271 their interactions while the ability to find interaction between the variables is not possible using PSO. In the
 272 beginning of optimization experiments, the understanding the process technique and function settings might
 273 be complex. The methodology used in this study, however, was easy to implement and the software used was
 274 free, open source, and user-friendly, which reduced the initial difficulty. Therefore, PSO was demonstrated
 275 to be an effective and highly accurate prediction technique for finding the initial optimum parameters for
 276 rPET90//rHDPE10 material for FGF/FPF.

277 Based on the result, it is evident that the optimal parameters for printing may vary depending on the object
 278 and each parameter has its own variation. One possible hypothesis is that the geometry of the object could
 279 influence the assignment of parameters and this effect might be more noticeable in large printings, yet further
 280 investigation is required to confirm this hypothesis. There are several physical mechanisms at play that are
 281 expected to alter the optimal printing parameters based on size and geometry of the object. For example, the
 282 cooling time and temperature history of a voxel will depend on the geometry of the printed object (Cleeman
 283 et al., 2022). Thus, to maintain a consistent thermal history the printing parameters must be adjusted as the
 284 geometry changes. This thermal history can also have more subtle effects, such as impacting the degree of

Table 3: Ideal printing parameters for fused granule fabrication of waste PET and HDPE blend made from shredded whole plastic water bottles

Variable	Line value	Planes value	Cube value	Δ	Units
T1	258	263	264	6 ±3.2	°C
Tb	86	82	84	4±2	°C
Ps	21	14	10	11±5.6	mm/s
E	1.07	0.87	1.32	0.5±0.3	-

285 crystallization even in the case of PLA ([Wijnen et al., 2018](#)).

286 In addition, the effects of material extrusion are magnified with scale, including the impact of thermal
 287 expansion and contraction. Small changes in contraction during cooling may cause acceptable distortions
 288 for small prints, but these are magnified for larger prints (e.g. causing deformation and in the worst cases
 289 delamination or loss of bed adhesion)([Shah et al., 2019](#)). Although, Roschli et al. ([2019](#)) showed the obstacles
 290 and possible solutions of the large-scale AM according to the way the parts are designed the incidence of the
 291 geometry in the printing parameters needs far more detailed future studies. Specifically better models for
 292 mapping 3-D printing parameter optimization of small printed objects to large-volume objects are needed.

293 Functional object print

294 The final parameters for print the case study product were determined based on the ideal paraeters found
 295 for the cube geometry.However, the print speed was ajusted to decrease the printing time and prevent
 296 delamination. This adjustment was made in accordance with the PSO results, which indicated that the
 297 material can be printed at a speed range of 10 to 20 mm/s. Increasing the printing speed reduces the cooling
 298 time between the layers,thereby minimizing the risk of delamination ([Roschli et al., 2019](#)), This is particularly
 299 important for larger objects, as delamination tends to be more pronounced in such cases.

300 The Gigabot X successfully produced a piece of furniture from multi-material recycled water bottles that
 301 included mixing HDPE and PET as shown in Figure [10 a](#).

302 The printing quality is acceptable as a prototype, proving the machine's capacity to print large-scale functional
 303 objects. The chair was able to comfortably hold a child with a mass of 20 kg, as shown in Figure [10 f](#). However,
 304 further evaluation is needed for the material used in the printing process. the printed object showed weak
 305 bond strength between the adjacent layers resulting in delamination, as seen in Figure [10 b](#) . This could
 306 be attributed to the difference in chemical properties of the materials, their immiscibility ([Chu et al., 2022](#);
 307 [William et al., 2021](#)), high crystallinity ([Verma et al., 2023](#)) and the large volume of the object as delamination
 308 issues were more prominent during the printing of the chair compared to the parameters optimization process.
 309 The delamination observed in larger objects can be attributed to the rapid cooling of the layers before the

material is once again deposited. This is in contrast to cube printing, where the smaller surface area allows better layer adhesion before complete cooling. Even popular 3-D printing materials like PLA can be affected by this issue, as observed from the print surface (Wijnen et al., 2018). To address the delamination problem and improve material properties, the addition of agents that reduce could be beneficial (Dai et al., 1997; Inoya et al., 2012; Kramer et al., 1994). This can enhance interfacial bonds through polymer modification (Gao et al., 2021) and viscosity reduction (Ko et al., 2019). Additionally, we observed printing warping problems (Figure 10 c), which are likely caused by the high crystallization rates of HDPE (Schirmeister et al., 2019). We tested the use of Magigoo adhesive (Thought3D Ltd., Paola, Malta) and the addition of a brim to improve bed adhesion, yet these solutions did not completely resolve the problem. A previous study showed that the use of a building plate made of thermoplastic elastomer SEBS allowed the adhesion of the plastic and facilitated easy detachment of the printed object without any breakage or damage [(schirmeister2019.This?) suggests a potential solution that should be further evaluated in future work. Another visible issue present in the close angles of the printed object was the shrinkage (Figure 10 d) which occurs during solidification and particularly upon polymer crystallization. Moreover, it is well-known that PET has hygroscopic tendencies and easily absorbs moisture from the temperature, which makes it difficult to extrude (Bustos Seibert et al., 2022). As a result, it is likely to break down in the presence of water, lowering the quality of the print. Prior to printing the chair some samples exhibited brittle behavior and void formation therefore, the material was consistently dried and the hopper was kept closed to prevent moisture from entering the environment. These measures helped to ensure a more suitable material for printing. Additionally, there are visible vibration and ringing problems (Figure 10 e) caused by the machine upgrades. Both acceleration and jerk (the maximum value of instantaneous speed change) require finer tuning to resolve these issues.

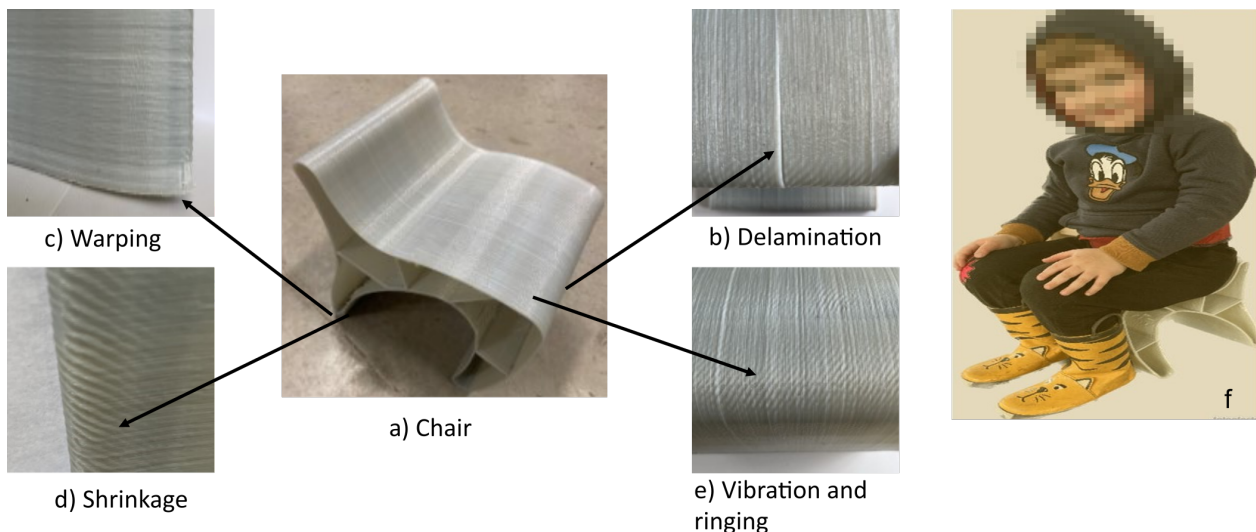


Figure 10: Finished children's chair and printing issues

331 **Cost and environmental impact**

332 The printing process took 10 hours and the printed object weighs 840 grams. Due to the found optimized
333 speed being low, the printing rate (grams per hour) is low considering the machine that pellet printers have
334 a typical throughput of 220 g to 9 kg per hour. To improve the printing time, upgrading the the extruder
335 motor to a more powerful would be benefitial. Besides, the energy required for 10 hours of 3-D printing was
336 found to be 6 kW-hr resulting in a production cost of ~1.2 € in function of the electricity cost in France, and
337 does not include the material cost, as the bottles used were obtained from post-consumer waste. When labor
338 costs are not included, the price was significant reduced (~88%) compared to the low-cost options available
339 in the market.

340 The economics of fabricating the case study product remained competitive even when using recycled plastic
341 pellets or shreds, which are available on the market for prices ranging from 1-10 €/kg. However, it is important
342 to note that labor, maintenance, and machine devaluation were not considered in the final price. These factors
343 should be considered in future work to ensure a comprehensive economic evaluation.

344 Regarding the environmental impact, this study does not evaluate the entire life cycle of the printed object.
345 However, various scientific studies have already shown the feasibility of distributed recycling ([Kerdlap et al., 2022](#); [Santander et al., 2020](#)). A comparison between conventional and distributed manufacturing in
346 terms of energy consumption and emissions has been conducted ([Kreiger and Pearce, 2013](#)). Other studies
347 have examined the environmental performance of AM ([Colorado et al., 2020](#); [Garcia et al., 2018](#)) and the
348 appearance of DRAM as a source of raw material for diverse 3-D printers coming from post-consumer plastic
349 waste in the form of either filament ([Hart et al., 2018](#); [Mikula et al., 2021](#); [Mohammed et al., 2017b](#); [Pakkanen et al., 2017b](#)) or granules ([Alexandre et al., 2020](#)).

352 Additionally, Caceres-Mendoza et al. ([2023](#)) have developed a comprehensive life cycle assessment of a DRAM
353 system focusing on the production of PLA filament, comparing virgin and recycled materials. The findings of
354 their environmental analysis revealed a analysis revealed a reduction of approximately 97% in the production
355 impacts, including climate change, fossil depletion, water depletion, and potential eutrophication, when using
356 recycled filament as opposed to virgin filament. It is important to note that these results are subject to the
357 energy supply and might vary depending on the geographical location.

358 **Conclusion and future work**

359 This study examined the feasibility of using mixed post-consumer waste as a feedstock material for direct 3-D
360 printing without the need of compatibilization. The results demostrated the potential of mixing solid waste
361 plastics (PET/HDPE) to be used as feedstock material, as evidenced by successfully printing a water bottle

³⁶² using two incompatible polymers from the cap and body of the bottle. Additionally, the results found that
³⁶³ a large-scale FGF 3-D printer was capable of producing cost-effective functional object using these mixed
³⁶⁴ waste PET/HDPE plastics. However, further research is necessary to analyze the mechanical properties of
³⁶⁵ the material and explore the use of compatibilizers that can enhance the interphase tension between plastics
³⁶⁶ and reduce their crystallinity. These measures could potentially improve and enhance the properties of both
³⁶⁷ the material and the 3-D printed parts.

³⁶⁸ These considerations become increasingly important as the size of the 3-D printed part increases. The
³⁶⁹ improvement of the material science of this approach can also offer an opportunity to improve the quality of
³⁷⁰ the printing time, reduce energy consumption of the machine, and improve the economic viability of DRAM
³⁷¹ using mixed plastic waste.

³⁷² In addition, future work could assess the different combinations or blends of commodity plastics with or with-
³⁷³ out the use of compatibilizers, to determine their printability. This investigation could lead to the elimination
³⁷⁴ of the selection/sorting process. In the same way, the development of a methodology that ensure process
³⁷⁵ reproducibility, even in areas with limited infrastructure opens up the potential for plastic revalorization
³⁷⁶ using DRAM.

³⁷⁷ Declaration of competing

³⁷⁸ The authors declare that they have no known competing financial interests or personal relationships that
³⁷⁹ could have appeared to influence the work reported in this paper.

³⁸⁰ Acknowledgments

³⁸¹ This project has received funding from the European Union's Horizon 2020 research and innovation program
³⁸² under grant agreement No 869952. The authors thank the LUE program for the financing of the thesis, the
³⁸³ Lorraine Fab Living lab platform and the Thompson endowment.

384 References

- 385 Alexandre, A., Cruz Sanchez, F.A., Boudaoud, H., Camargo, M., Pearce, J.M., 2020. Mechanical Properties
386 of Direct Waste Printing of Polylactic Acid with Universal Pellets Extruder: Comparison to Fused
387 Filament Fabrication on Open-Source Desktop Three-Dimensional Printers. *3D Printing and Additive
388 Manufacturing* 7, 237–247. <https://doi.org/10.1089/3dp.2019.0195>
- 389 Anderson, I., 2017. Mechanical Properties of Specimens 3D Printed with Virgin and Recycled Polylactic
390 Acid. *3D Printing and Additive Manufacturing* 4, 110–115. <https://doi.org/10.1089/3dp.2016.0054>
- 391 Asadi-Eydivand, M., Solati-Hashjin, M., Fathi, A., Padashi, M., Abu Osman, N.A., 2016. Optimal design
392 of a 3D-printed scaffold using intelligent evolutionary algorithms. *Applied Soft Computing* 39, 36–47.
393 <https://doi.org/10.1016/j.asoc.2015.11.011>
- 394 Attaran, M., 2020. 3D Printing Role in Filling the Critical Gap in the Medical Supply Chain during COVID-
395 19 Pandemic. *American Journal of Industrial and Business Management* 10, 988–1001. <https://doi.org/10.4236/ajibm.2020.105066>
- 396 Baechler, C., DeVuono, M., Pearce, J.M., 2013. Distributed recycling of waste polymer into RepRap feedstock.
397 *Rapid Prototyping Journal* 19, 118–125. <https://doi.org/10.1108/13552541311302978>
- 398 Bowyer, A., 2014. 3D Printing and Humanity's First Imperfect Replicator. *3D Printing and Additive
399 Manufacturing* 1, 4–5. <https://doi.org/10.1089/3dp.2013.0003>
- 400 Bustos Seibert, M., Mazzei Capote, G.A., Gruber, M., Volk, W., Osswald, T.A., 2022. Manufacturing
401 of a PET Filament from Recycled Material for Material Extrusion (MEX). *Recycling* 7, 69. <https://doi.org/10.3390/recycling7050069>
- 402 Byard, D.J., Woern, A.L., Oakley, R.B., Fiedler, M.J., Snabes, S.L., Pearce, J.M., 2019. Green fab lab
403 applications of large-area waste polymer-based additive manufacturing. *Additive Manufacturing* 27, 515–
404 525. <https://doi.org/10.1016/j.addma.2019.03.006>
- 405 Caceres-Mendoza, C., Santander-Tapia, P., Cruz Sanchez, F.A., Troussier, N., Camargo, M., Boudaoud, H.,
406 2023. Life cycle assessment of filament production in distributed plastic recycling via additive manufac-
407 turing. *Cleaner Waste Systems* 5, 100100. <https://doi.org/10.1016/j.clwas.2023.100100>
- 408 Carrete, I.A., Quiñonez, P.A., Bermudez, D., Roberson, D.A., 2021. Incorporating Textile-Derived Cellulose
409 Fibers for the Strengthening of Recycled Polyethylene Terephthalate for 3D Printing Feedstock Materials.
410 *Journal of polymers and the environment*.
- 411 Chen, R.S., Ab Ghani, M.H., Salleh, M.N., Ahmad, S., Tarawneh, M.A., 2015. Mechanical, water absorption,
412 and morphology of recycled polymer blend rice husk flour biocomposites. *Journal of Applied Polymer
413 Science* 132. <https://doi.org/10.1002/app.41494>
- 414 Chong, S., Pan, G.-T., Khalid, M., Yang, T.C.-K., Hung, S.-T., Huang, C.-M., 2017. Physical Character-
415 ization and Pre-assessment of Recycled High-Density Polyethylene as 3D Printing Material. *Journal of
416 Polymers and the Environment* 25, 136–145. <https://doi.org/10.1007/s10924-016-0793-4>
- 417 Choong, Y.Y.C., Tan, H.W., Patel, D.C., Choong, W.T.N., Chen, C.-H., Low, H.Y., Tan, M.J., Patel, C.D.,
418 Chua, C.K., 2020. The global rise of 3D printing during the COVID-19 pandemic. *Nat Rev Mater* 5,
419 637–639. <https://doi.org/10.1038/s41578-020-00234-3>
- 420 Chu, J.S., Koay, S.C., Chan, M.Y., Choo, H.L., Ong, T.K., 2022. Recycled plastic filament made from post-
421 consumer expanded polystyrene and polypropylene for fused filament fabrication. *Polymer Engineering
422 & Science* 62, 3786–3795. <https://doi.org/10.1002/pen.26144>
- 423 Cleeman, J., Bogut, A., Mangrolia, B., Ripberger, A., Kate, K., Zou, Q., Malhotra, R., 2022. Scalable, Flex-
424 ible and Resilient Parallelization of Fused Filament Fabrication: Breaking Endemic Tradeoffs in Material
425 Extrusion Additive Manufacturing. *Additive Manufacturing* 102926. [https://doi.org/10.1016/J.ADDM A.2022.102926](https://doi.org/10.1016/J.ADDM
426 A.2022.102926)
- 427 Colorado, H.A., Velásquez, E.I.G., Monteiro, S.N., 2020. Sustainability of additive manufacturing: The circu-

- 430 lar economy of materials and environmental perspectives. *Journal of Materials Research and Technology*
431 9, 8221–8234. <https://doi.org/10.1016/j.jmrt.2020.04.062>
- 432 Corsini, L., Aranda-Jan, C.B., Moultrie, J., 2022. The impact of 3D printing on the humanitarian supply
433 chain. <https://doi.org/10.17863/CAM.51226>
- 434 Cruz Sanchez, F.A., Boudaoud, H., Camargo, M., Pearce, J.M., 2020. Plastic recycling in additive manu-
435 facturing: A systematic literature review and opportunities for the circular economy. *Journal of Cleaner
436 Production* 264, 121602. <https://doi.org/10.1016/j.jclepro.2020.121602>
- 437 Cruz Sanchez, F.A., Boudaoud, H., Hoppe, S., Camargo, M., 2017. Polymer recycling in an open-source
438 additive manufacturing context: Mechanical issues. *Additive Manufacturing* 17, 87–105. [https://doi.org/10.1016/j.addma.2017.05.013](https://doi.or-
439 g/10.1016/j.addma.2017.05.013)
- 440 Dai, C.-A., Jandt, K.D., Iyengar, D.R., Slack, N.L., Dai, K.H., Davidson, W.B., Kramer, E.J., Hui, C.-
441 Y., 1997. Strengthening Polymer Interfaces with Triblock Copolymers. *Macromolecules* 30, 549–560.
442 <https://doi.org/10.1021/ma960396s>
- 443 Dertinger, S.C., Gallup, N., Tanikella, N.G., Grasso, M., Vahid, S., Foot, P.J.S., Pearce, J.M., 2020. Technical
444 pathways for distributed recycling of polymer composites for distributed manufacturing: Windshield wiper
445 blades. *Resources, Conservation and Recycling* 157, 104810. [https://doi.org/10.1016/j.resconrec.2020.1-04810](https://doi.org/10.1016/j.resconrec.2020.1-
446 04810)
- 447 Despesse, M., Baumers, M., Brown, P., Charnley, F., Ford, S.J., Garmulewicz, A., Knowles, S., Minshall,
448 T.H.W., Mortara, L., Reed-Tsochas, F.P., Rowley, J., 2017. Unlocking value for a circular economy
449 through 3D printing: A research agenda. *Technological Forecasting and Social Change* 115, 75–84. [https://doi.org/10.1016/j.techfore.2016.09.021](https://
450 //doi.org/10.1016/j.techfore.2016.09.021)
- 451 Evode, N., Qamar, S.A., Bilal, M., Barceló, D., Iqbal, H.M.N., 2021. Plastic waste and its management
452 strategies for environmental sustainability. *Case Studies in Chemical and Environmental Engineering* 4,
453 100142. <https://doi.org/10.1016/j.cscee.2021.100142>
- 454 Fontana, L., Giubilini, A., Arrigo, R., Malucelli, G., Minetola, P., 2022. Characterization of 3D Printed Poly-
455 lactic Acid by Fused Granular Fabrication through Printing Accuracy, Porosity, Thermal and Mechanical
456 Analyses. *Polymers* 14, 3530. <https://doi.org/10.3390/polym14173530>
- 457 Ford, S., Despesse, M., 2016. Additive manufacturing and sustainability: An exploratory study of the
458 advantages and challenges. *Journal of Cleaner Production* 137, 1573–1587. [https://doi.org/10.1016/j.jc-lepro.2016.04.150](https://doi.org/10.1016/j.jc-
459 lepro.2016.04.150)
- 460 Gaikwad, V., Ghose, A., Cholake, S., Rawal, A., Iwato, M., Sahajwalla, V., 2018. Transformation of E-
461 Waste Plastics into Sustainable Filaments for 3D Printing. *ACS Sustainable Chemistry & Engineering* 6,
462 14432–14440. <https://doi.org/10.1021/acssuschemeng.8b03105>
- 463 Gallup, N., Bow, J.K., Pearce, J.M., 2018. Economic Potential for Distributed Manufacturing of Adaptive
464 Aids for Arthritis Patients in the U.S. *Geriatrics* 3, 89. <https://doi.org/10.3390/geriatrics3040089>
- 465 Gao, X., Qi, S., Kuang, X., Su, Y., Li, J., Wang, D., 2021. Fused filament fabrication of polymer materials:
466 A review of interlayer bond. *Additive Manufacturing* 37, 101658. [https://doi.org/10.1016/j.addma.2020.101658](https://doi.org/10.1016/j.addma.2020.
467 .101658)
- 468 Garcia, F.L., Moris, V.A. da S., Nunes, A.O., Silva, D.A.L., 2018. Environmental performance of additive
469 manufacturing process – an overview. *Rapid Prototyping Journal* 24, 1166–1177. [https://doi.org/10.1108/RPJ-05-2017-0108](https://doi.org/10.110-
470 8/RPJ-05-2017-0108)
- 471 Geyer, R., 2020. Chapter 2 - Production, use, and fate of synthetic polymers, in: Letcher, T.M. (Ed.), *Plastic
472 Waste and Recycling*. Academic Press, pp. 13–32. <https://doi.org/10.1016/B978-0-12-817880-5.00002-5>
- 473 Geyer, R., Jambeck, J.R., Law, K.L., 2017. Production, use, and fate of all plastics ever made. *Science
474 Advances* 3, e1700782. <https://doi.org/10.1126/sciadv.1700782>
- 475 Grassi, G., Spagnolo, S.L., Paoletti, I., 2019. Fabrication and durability testing of a 3D printed façade for

- 476 desert climates. *Additive Manufacturing* 28, 439.
- 477 Gwamuri, J., Franco, D., Khan, K.Y., Gauchia, L., Pearce, J.M., 2016. High-Efficiency Solar-Powered 3-D
478 Printers for Sustainable Development. *Machines* 4, 3. <https://doi.org/10.3390/machines4010003>
- 479 Hart, K.R., Frketic, J.B., Brown, J.R., 2018. Recycling meal-ready-to-eat (MRE) pouches into polymer
480 filament for material extrusion additive manufacturing. *Additive Manufacturing* 21, 536–543. <https://doi.org/10.1016/j.addma.2018.04.011>
- 481 ImageJ, 2023. Image processing and analysis in java [WWW Document]. URL <https://imagej.nih.gov/ij/do wnload.html> (accessed 6.13.2023).
- 482 Inoya, H., Wei Leong, Y., Klinklai, W., Thumsorn, S., Makata, Y., Hamada, H., 2012. Compatibilization
483 of recycled poly (ethylene terephthalate) and polypropylene blends: Effect of polypropylene molecular
484 weight on homogeneity and compatibility. *Journal of applied polymer science* 124, 3947–3955.
- 485 Jaisingh Sheoran, A., Kumar, H., 2020. Fused Deposition modeling process parameters optimization and
486 effect on mechanical properties and part quality: Review and reflection on present research. *Materials
487 Today: Proceedings, International Conference on Mechanical and Energy Technologies* 21, 1659–1672.
488 <https://doi.org/10.1016/j.matpr.2019.11.296>
- 489 Jonathan GUIDIGO1, Stéphane MOLINA2, Edmond C. ADJOVI3, André MERLIN 4, DONNOT André5,
490 Merlin SIMO TAGNE6, 2017. Polyethylene Low and High Density-Polyethylene Terephthalate and
491 Polypropylene Blend as Matrices for Wood Flour, in: *International Journal of Science and Research
492 (IJSR)*. pp. 1069–1074. <https://doi.org/10.21275/ART20164296>
- 493 Jones, R., Haufe, P., Sells, E., Iravani, P., Olliver, V., Palmer, C., Bowyer, A., 2011. RepRap – the replicating
494 rapid prototyper. *Robotica* 29, 177–191. <https://doi.org/10.1017/S026357471000069X>
- 495 Kerlap, P., Purnama, A.R., Low, J.S.C., Tan, D.Z.L., Barlow, C.Y., Ramakrishna, S., 2022. Comparing the
496 environmental performance of distributed versus centralized plastic recycling systems: Applying hybrid
497 simulation modeling to life cycle assessment. *Journal of Industrial Ecology* 26, 252–271. <https://doi.org/10.1111/jiec.13151>
- 498 King, D., Babasola, A., Rozario, J., Pearce, J., 2014. Mobile Open-Source Solar-Powered 3-D Printers for
499 Distributed Manufacturing in Off-Grid Communities. *Challenges in Sustainability* 2. <https://doi.org/10.12924/cis2014.02010018>
- 500 Ko, Y.S., Herrmann, D., Tolar, O., Elspass, W.J., Brändli, C., 2019. Improving the filament weld-strength of
501 fused filament fabrication products through improved interdiffusion. *Additive Manufacturing* 29, 100815.
502 <https://doi.org/10.1016/j.addma.2019.100815>
- 503 Kramer, E.J., Norton, L.J., Dai, C.-A., Sha, Y., Hui, C.-Y., 1994. Strengthening polymer interfaces. *Faraday
504 Discussions* 98, 31–46. <https://doi.org/10.1039/FD9949800031>
- 505 Kratofil, L., Hrnjak-Murgić, Z., Jelencć, J., Andrićć, B., Kovacć, T., Merzel, V., 2006. Study of the compati-
506 bility effect on blends prepared from waste poly (ethylene-terephthalate) and high density polyethylene.
507 *International Polymer Processing* 21, 328–335.
- 508 Kreiger, M.A., Mulder, M.L., Glover, A.G., Pearce, J.M., 2014. Life cycle analysis of distributed recycling
509 of post-consumer high density polyethylene for 3-D printing filament. *Journal of Cleaner Production* 70,
510 90–96. <https://doi.org/10.1016/j.jclepro.2014.02.009>
- 511 Kreiger, M., Pearce, J.M., 2013. Environmental Impacts of Distributed Manufacturing from 3-D Printing of
512 Polymer Components and Products. *MRS Proceedings* 1492, 85–90. <https://doi.org/10.1557/opr.2013.319>
- 513 Langer, E., Bortel, K., Waskiewicz, S., Lenartowicz-Klik, M., 2020. Methods of PET Recycling, Plasticizers
514 Derived from Post-Consumer PET. <https://doi.org/10.1016/b978-0-323-46200-6.00005-2>
- 515 Lei, Y., Wu, Q., Zhang, Q., 2009. Morphology and properties of microfibrillar composites based on recycled
516 poly (ethylene terephthalate) and high density polyethylene. *Composites Part A: Applied Science and
517 Technology* 40, 103–108.

- 522 Manufacturing 40, 904–912. <https://doi.org/10.1016/j.compositesa.2009.04.017>
- 523 Lipsky, S., Przyjemski, A., Velasquez, M., Gershenson, J., 2019. 3D Printing for Humanitarian Relief:
524 The Printer Problem, in: 2019 IEEE Global Humanitarian Technology Conference (GHTC). pp. 1–7.
525 <https://doi.org/10.1109/GHTC46095.2019.9033053>
- 526 Little, H.A., Tanikella, N.G., J. Reich, M., Fiedler, M.J., Snabes, S.L., Pearce, J.M., 2020. Towards Dis-
527 tributed Recycling with Additive Manufacturing of PET Flake Feedstocks. Materials 13, 4273. <https://doi.org/10.3390/ma13194273>
- 528 Löschke, S.K., Mai, J., Proust, G., Brambilla, A., 2019. Microtimber: The Development of a 3D Printed
529 Composite Panel Made from Waste Wood and Recycled Plastics. Digital Wood Design 24, 827–848.
530 https://doi.org/10.1007/978-3-030-03676-8_33
- 531 MacArthur, E., 2017. Beyond plastic waste. Science 358, 843–843. <https://doi.org/10.1126/science.aa06749>
- 532 Mikula, K., Skrzypczak, D., Izdyorczyk, G., Warchał, J., Moustakas, K., Chojnacka, K., Witek-Krowiak,
533 A., 2021. 3D printing filament as a second life of waste plastics—a review. Environmental Science and
534 Pollution Research 28, 12321–12333. <https://doi.org/10.1007/s11356-020-10657-8>
- 535 Mohammed, M.I., Das, A., Gomez-Kervin, E., Wilson, D., Gibson, I., 2017a. EcoPrinting: Investigating the
536 Use of 100% Recycled Acrylonitrile Butadiene Styrene (ABS) for Additive Manufacturing. University of
537 Texas at Austin.
- 538 Mohammed, M.I., Mohan, M., Das, A., Johnson, M.D., Badwal, P.S., McLean, D., Gibson, I., 2017b. A low
539 carbon footprint approach to the reconstitution of plastics into 3D-printer filament for enhanced waste
540 reduction. KnE Engineering 234–241. <https://doi.org/10.18502/keg.v2i2.621>
- 541 Mohammed, M.I., Wilson, D., Gomez-Kervin, E., Rosson, L., Long, J., 2018. EcoPrinting: Investigation of
542 Solar Powered Plastic Recycling and Additive Manufacturing for Enhanced Waste Management and Sus-
543 tainable Manufacturing, in: 2018 IEEE Conference on Technologies for Sustainability (SusTech). IEEE,
544 pp. 1–6. <https://doi.org/10.1109/SusTech.2018.8671370>
- 545 Nofar, M., Oğuz, H., 2019. Development of PBT/Recycled-PET Blends and the Influence of Using Chain
546 Extender. Journal of Polymers and the Environment 27, 1404–1417. <https://doi.org/10.1007/s10924-019-01435-w>
- 547 Novak, J.I., Loy, J., 2020. A critical review of initial 3D printed products responding to COVID-19 health and
548 supply chain challenges. Emerald Open Research 2, 24. <https://doi.org/10.35241/emeraldopenres.13697.1>
- 549 Oberloier, S., Whisman, N.G., Pearce, J.M., 2022a. Finding Ideal Parameters for Recycled Material Fused
550 Particle Fabrication-Based 3D Printing Using an Open Source Software Implementation of Particle Swarm
551 Optimization. 3D Printing and Additive Manufacturing. <https://doi.org/10.1089/3dp.2022.0012>
- 552 Oberloier, S., Whisman, N.G., Pearce, J.M., 2022b. Finding Ideal Parameters for Recycled Material Fused
553 Particle Fabrication-Based 3D Printing Using an Open Source Software Implementation of Particle Swarm
554 Optimization. 3D Printing and Additive Manufacturing. <https://doi.org/10.1089/3dp.2022.0012>
- 555 Pakkanen, J., Manfredi, D., Minetola, P., Iuliano, L., 2017a. About the Use of Recycled or Biodegradable
556 Filaments for Sustainability of 3D Printing, in: Campana, G., Howlett, R.J., Setchi, R., Cimatti, B.
557 (Eds.), Springer International Publishing, Cham, pp. 776–785. https://doi.org/10.1007/978-3-319-57078-5_73
- 558 Pakkanen, J., Manfredi, D., Minetola, P., Iuliano, L., 2017b. About the Use of Recycled or Biodegradable
559 Filaments for Sustainability of 3D Printing, in: Campana, G., Howlett, R.J., Setchi, R., Cimatti, B. (Eds.),
560 Sustainable Design and Manufacturing 2017, Smart Innovation, Systems and Technologies. Springer
561 International Publishing, Cham, pp. 776–785. https://doi.org/10.1007/978-3-319-57078-5_73
- 562 Pan, Y., Wu, G., Ma, H., Zhou, S., Zhang, H., 2020. Improved compatibility of PET/HDPE blend by using
563 GMA grafted thermoplastic elastomer. Polymer-Plastics Technology and Materials 59, 1887–1898.
- 564 Pearce, J., Qian, J.-Y., 2022. Economic Impact of DIY Home Manufacturing of Consumer Products with

- 568 Low-cost 3D Printing from Free and Open Source Designs. European Journal of Social Impact and
569 Circular Economy 3, 1–24. <https://doi.org/10.13135/2704-9906/6508>
- 570 Petersen, E., Kidd, R., Pearce, J., 2017. Impact of DIY Home Manufacturing with 3D Printing on the Toy
571 and Game Market. Technologies 5, 45. <https://doi.org/10.3390/technologies5030045>
- 572 Petsiuk, A., Lavu, B., Dick, R., Pearce, J.M., 2022. Waste Plastic Direct Extrusion Hangprinter. Inventions
573 7, 70. <https://doi.org/10.3390/inventions7030070>
- 574 Pringle, A.M., Rudnicki, M., Pearce, J.M., 2018. Wood Furniture Waste-Based Recycled 3-D Printing
575 Filament. Forest Products Journal 68, 86–95. <https://doi.org/10.13073/FPJ-D-17-00042>
- 576 Raju, M., Gupta, M.K., Bhanot, N., Sharma, V.S., 2019. A hybrid PSO-BFO evolutionary algorithm for
577 optimization of fused deposition modelling process parameters. Journal of Intelligent Manufacturing 30,
578 2743–2758. <https://doi.org/10.1007/s10845-018-1420-0>
- 579 Rattan, R.S., Nauta, N., Romani, A., Pearce, J.M., 2023. Hangprinter for large scale additive manufacturing
580 using fused particle fabrication with recycled plastic and continuous feeding. HardwareX 13, e00401.
581 <https://doi.org/10.1016/j.hwx.2023.e00401>
- 582 Reich, M.J., Woern, A.L., Tanikella, N.G., Pearce, J.M., 2019. Mechanical Properties and Applications of
583 Recycled Polycarbonate Particle Material Extrusion-Based Additive Manufacturing. Materials 12, 1642.
584 <https://doi.org/10.3390/ma12101642>
- 585 Rett, J.P., Traore, Y.L., Ho, E.A., 2021. Sustainable Materials for Fused Deposition Modeling 3D Printing
586 Applications. Advanced Engineering Materials 23, 2001472. <https://doi.org/10.1002/adem.202001472>
- 587 Romani, A., Rognoli, V., Levi, M., 2021. Design, Materials, and Extrusion-Based Additive Manufacturing
588 in Circular Economy Contexts: From Waste to New Products. Sustainability 13, 7269. <https://doi.org/10.3390/su13137269>
- 589 Roschli, A., Gaul, K.T., Boulger, A.M., Post, B.K., Chesser, P.C., Love, L.J., Blue, F., Borish, M., 2019.
590 Designing for Big Area Additive Manufacturing. Additive Manufacturing 25, 275–285. <https://doi.org/10.1016/j.addma.2018.11.006>
- 591 Saad, M.S., Nor, A.M., Baharudin, M.E., Zakaria, M.Z., Aimani, A.F., 2019. Optimization of surface rough-
592 ness in FDM 3D printer using response surface methodology, particle swarm optimization, and symbiotic
593 organism search algorithms. The International Journal of Advanced Manufacturing Technology 105,
594 5121–5137. <https://doi.org/10.1007/s00170-019-04568-3>
- 595 Salmi, M., Akmal, J.S., Pei, E., Wolff, J., Jaribion, A., Khajavi, S.H., 2020. 3D Printing in COVID-19:
596 Productivity Estimation of the Most Promising Open Source Solutions in Emergency Situations. Applied
597 Sciences 10, 4004. <https://doi.org/10.3390/app10114004>
- 598 Santander, P., Cruz Sanchez, F.A., Boudaoud, H., Camargo, M., 2020. Closed loop supply chain network for
599 local and distributed plastic recycling for 3D printing: A MILP-based optimization approach. Resources,
600 Conservation and Recycling 154, 104531. <https://doi.org/10.1016/j.resconrec.2019.104531>
- 601 Savonen, B.L., Mahan, T.J., Curtis, M.W., Schreier, J.W., Gershenson, J.K., Pearce, J.M., 2018. De-
602 velopment of a Resilient 3-D Printer for Humanitarian Crisis Response. Technologies 6, 30. <https://doi.org/10.3390/technologies6010030>
- 603 Schirmeister, C.G., Hees, T., Licht, E.H., Mülhaupt, R., 2019. 3D printing of high density polyethylene by
604 fused filament fabrication. Additive Manufacturing 28, 152–159. <https://doi.org/10.1016/j.addma.2019.05.003>
- 605 Sells, E., Smith, Z., Bailard, S., Bowyer, A., Olliver, V., 2009. RepRap: The Replicating Rapid Prototyper
606 - maximizing customizability by breeding the means of production, in: Piller, F.T., Tseng, M.M. (Eds.),
607 Handbook of Research in Mass Customization and Personalization. World Scientific, pp. 568–580.
- 608 Selvam, A., Mayilswamy, S., Whenish, R., 2020. Strength Improvement of Additive Manufacturing Compo-
609 nents by Reinforcing Carbon Fiber and by Employing Bioinspired Interlock Sutures. Journal of Vinyl
610

- and Additive Technology 26, 511–523. <https://doi.org/10.1002/vnl.21766>
- Shah, J., Snider, B., Clarke, T., Kozutsky, S., Lacki, M., Hosseini, A., 2019. Large-scale 3D printers for additive manufacturing: Design considerations and challenges. The International Journal of Advanced Manufacturing Technology 104, 3679–3693. <https://doi.org/10.1007/s00170-019-04074-6>
- Shirmohammadi, M., Goushchi, S.J., Keshtiban, P.M., 2021. Optimization of 3D printing process parameters to minimize surface roughness with hybrid artificial neural network model and particle swarm algorithm. Progress in Additive Manufacturing 6, 199–215. <https://doi.org/10.1007/s40964-021-00166-6>
- Siltaloppi, J., Jähi, M., 2021. Toward a sustainable plastics value chain: Core conundrums and emerging solution mechanisms for a systemic transition. Journal of Cleaner Production 315, 128113. <https://doi.org/10.1016/j.jclepro.2021.128113>
- Soares, J., Miguel, I., Venâncio, C., Lopes, I., Oliveira, M., 2021. Public views on plastic pollution: Knowledge, perceived impacts, and pro-environmental behaviours. Journal of Hazardous Materials 412, 125227. <https://doi.org/10.1016/j.jhazmat.2021.125227>
- Taghavi, S.K., Shahrajabian, H., Hosseini, H.M., 2018. Detailed comparison of compatibilizers MAPE and SEBS-g-MA on the mechanical/thermal properties, and morphology in ternary blend of recycled PET/HDPE/MAPE and recycled PET/HDPE/SEBS-g-MA. Journal of Elastomers & Plastics 50, 13–35.
- Van de Voorde, B., Katalagarianakis, A., Huysman, S., Toncheva, A., Raquez, J.-M., Duretek, I., Holzer, C., Cardon, L., Bernaerts, K., V, Van Hemelrijck, D., Pyl, L., Van Vlierberghe, S., 2022. Effect of extrusion and fused filament fabrication processing parameters of recycled poly(ethylene terephthalate) on the crystallinity and mechanical properties. Additive Manufacturing 50. <https://doi.org/10.1016/j.addma.2021.102518>
- Vaucher, J., Demongeot, A., Michaud, V., Leterrier, Y., 2022. Recycling of Bottle Grade PET: Influence of HDPE Contamination on the Microstructure and Mechanical Performance of 3D Printed Parts. Polymers 14, 5507. <https://doi.org/10.3390/polym14245507>
- Verma, N., Awasthi, P., Gupta, A., Banerjee, S.S., 2023. Fused Deposition Modeling of Polyolefins: Challenges and Opportunities. Macromolecular Materials and Engineering 308, 2200421. <https://doi.org/10.1002/mame.202200421>
- Wijnen, B., Sanders, P., Pearce, J.M., 2018. Improved model and experimental validation of deformation in fused filament fabrication of polylactic acid. Progress in Additive Manufacturing 3, 193–203. <https://doi.org/10.1007/s40964-018-0052-4>
- William, L.J.W., Koay, S.C., Chan, M.Y., Pang, M.M., Ong, T.K., Tshai, K.Y., 2021. Recycling Polymer Blend made from Post-used Styrofoam and Polypropylene for Fuse Deposition Modelling. Journal of Physics: Conference Series 2120, 012020. <https://doi.org/10.1088/1742-6596/2120/1/012020>
- Woern, A.L., McCaslin, J.R., Pringle, A.M., Pearce, J.M., 2018. RepRapable Recyclebot: Open source 3-D printable extruder for converting plastic to 3-D printing filament. HardwareX 4, e00026. <https://doi.org/10.1016/j.ohx.2018.e00026>
- Wong, J.Y., 2015. Ultra-Portable Solar-Powered 3D Printers for Onsite Manufacturing of Medical Resources. Aerospace Medicine and Human Performance 86, 830–834. <https://doi.org/10.3357/AMHP.4308.2015>
- Zander, N.E., Gillan, M., Burckhard, Z., Gardea, F., 2019. Recycled polypropylene blends as novel 3D printing materials. Additive Manufacturing 25, 122–130. <https://doi.org/10.1016/j.addma.2018.11.009>
- Zander, N.E., Gillan, M., Lambeth, R.H., 2018. Recycled polyethylene terephthalate as a new FFF feedstock material. Additive Manufacturing 21, 174–182. <https://doi.org/10.1016/j.addma.2018.03.007>
- Zhang, Y., Wang, S., Ji, G., 2015. A Comprehensive Survey on Particle Swarm Optimization Algorithm and Its Applications. Mathematical Problems in Engineering 2015, e931256. <https://doi.org/10.1155/2015/931256>
- Zhong, S., Pearce, J.M., 2018. Tightening the loop on the circular economy: Coupled distributed recycling

⁶⁶⁰ and manufacturing with recyclebot and RepRap 3-D printing. Resources, Conservation and Recycling
⁶⁶¹ 128, 48–58. <https://doi.org/10.1016/j.resconrec.2017.09.023>